

Notes

Metal Complexes of *N-p*-Nitrobenzoylamido-*meso*-tetraphenylporphyrin: *cis*-Acetato-*N-p*-nitrobenzoylimido-*meso*- tetraphenylporphyrinatothallium(III) and *N-p*-Nitrobenzoylimido-*meso*- tetraphenylporphyrinatonicel(II)

Chen-Shing Chang, Ching-Huei Chen, Yu-I Li,
Bing-Chuang Liao, Bao-Tsan Ko,
Shanmugam Elango, and Jyh-Horung Chen*

Department of Chemistry, National Chung-Hsing University,
Taichung 40227, Taiwan, R.O.C.

Lian-Pin Hwang

Department of Chemistry, National Taiwan University and
Institute of Atomic and Molecular Sciences,
Academia Sinica, Taipei 10764, Taiwan, R.O.C.

Received July 24, 2000

Introduction

Metalloporphyrins with a bridged structure between the central metal and one of the four pyrrole nitrogens have drawn much attention in recent times. Bridged metalloporphyrins with only metal–NTs–N linkages (metal = Zn,¹ Ni,² Fe,³ Hg,⁴ Ga,⁵ Tl,⁵ Ts = tosyl) have so far been reported. Callot et al.² reported the synthesis and ¹H NMR investigation of the metalation of *N-p*-nitrobenzoylamido-*meso*-tetraphenylporphyrin [*N-p*-HNCOC₆H₄NO₂-Htpp] (tpp = dianion of *meso*-tetraphenylporphyrin) leading to mononuclear complexes of *N-p*-nitrobenzoylimido-*meso*-tetraphenylporphyrinatonicel(II) Ni(*N-p*-NCOC₆H₄NO₂-tpp) (**1**) and *N-p*-nitrobenzoylimido-*meso*-tetraphenylporphyrinatocopper(II) Cu(*N-p*-NCOC₆H₄NO₂-tpp) (**2**).

There are no X-ray structural data available for the metal ion [M(II) and M(III)] complexes of HNCOC₆H₄NO₂-Htpp. In this paper, we report the X-ray structural determination of the title compound Ni(*N-p*-NCOC₆H₄NO₂-tpp) (**1**), and we also present the results upon replacing Ni(II) with Tl(III) in **1** forming a new compound (**3**). This replacement increases the coordination number (CN) from 4 for **1** to 6 for *cis*-acetato-*N-p*-nitrobenzoylimido-*meso*-tetraphenylporphyrinatothallium(III) Tl(*N-p*-NCOC₆H₄NO₂-tpp)(OAc) (**3**). The presence of acetate ligands in **3** plays a role in somewhat artificially increasing the coordination number. Because of the larger size of the Tl³⁺ (*r*_{ion}

= 1.025 Å),⁶ the relative position of OAc[−] and *p*-nitrobenzoyl (NB) group coordinated to the Tl atom might lead to a *cis* configuration in **3**. In addition, the acetate exchange of Tl(*N*-NTs-tpp)(OAc) observed in CD₂Cl₂ prompted us to investigate a similar intermolecular exchange for complex **3** in THF-*d*₈ by ¹H and ¹³C dynamic NMR method.⁵

Experimental Section

Ni(*N-p*-NCOC₆H₄NO₂-tpp) (**1**).² Compound **1** was dissolved in CH₂Cl₂ and layered with MeOH, and thus the purple crystals of **1** were obtained for single-crystal X-ray analysis. ¹H NMR (599.95 MHz, CDCl₃, 25 °C): δ 8.99 [d, H_β(18,39), ³J(H–H) = 4.8 Hz], H_β(a,b) represents the two equivalent β-pyrrole protons attached to carbons a and b, respectively; 8.72[s, H_β(28,29)]; 8.68 [d, H_β(17,40), ³J(H–H) = 4.8 Hz]; 7.66–8.14 (m, phenyl protons); 7.57 [s, H_β(50,51)]; 6.80 [d, H_{NB}(4,6) or NB-H_{3,5}, ³J(H–H) = 9.0 Hz], H_{NB}(c,d) represents the two equivalent protons attached to carbons c and d of *p*-nitrobenzoyl (NB) group, respectively; 4.93 [d, H_{NB}(3,7) or NB-H_{2,6}, ³J(H–H) = 9.0 Hz].

Tl(*N-p*-NCOC₆H₄NO₂-tpp)(OAc) (**3**). A mixture of *N-p*-HNCOC₆H₄NO₂-Htpp (50 mg, 0.0068 mmol) in CH₂Cl₂ (10 cm³) and Tl(OAc)₃ (40 mg, 0.12 mmol) in MeOH (2.5 cm³) was refluxed for 1 h. After concentrating, the residue was dissolved in CHCl₃, dried with anhydrous Na₂SO₄, and filtered. The filtrate was concentrated and recrystallized from CH₂Cl₂–MeOH [1:5 (v/v)] yielding purple solid of **3** (39 mg, 0.037 mmol, 55%) which was again dissolved in CH₂Cl₂–ether [1:1 (v/v)] and layered with MeOH to get purple crystals for single-crystal X-ray analysis. ¹H NMR (599.95 MHz, CD₂Cl₂, 25 °C): δ 9.32 [d d, H_β(8,17), ⁴J(Tl–H) = 20 Hz and ³J(H–H) = 4.5 Hz]; 8.96 [dd, H_β(7,18), ⁴J(Tl–H) = 14 Hz and ³J(H–H) = 4.8 Hz]; 8.63 [d, H_β(12,13), ⁴J(Tl–H) = 75.3 Hz]; 7.20 [d, H_β(2,3), ⁵J(Tl–H) = 6 Hz]; 8.50(m), 8.22 (m) and 8.12 (m) for phenyl ortho protons (*o*-H); 7.75–7.89 (m) for phenyl meta and para protons (*m*-, *p*-H); 7.04 [d, H_{NB}(48,50) or NB-H_{3,5}, ³J(H–H) = 8.4 Hz], 5.25 [t, H_{NB}(47,51) or NB-H_{2,6}, ³J(H–H) = 8.4 Hz]; 0.17 (s, OAc). MS, *m/z* (assignment, rel intensity): 1040 ([Tl(*N-p*-NCOC₆H₄NO₂-tpp)(OAc)]⁺, 1.65), 981 ([Tl(*N-p*-NCOC₆H₄NO₂-tpp)]⁺, 42.89), 817 ([Tl(tpp) + H]⁺, 23.28), 779 ([H-*N-p*-NCOC₆H₄NO₂-Htpp]⁺, 20.88), 614 (Htpp⁺, 16.99), 205 (²⁰⁵Tl⁺, 64.34), 203 (²⁰³Tl⁺, 26.22). UV/visible spectrum, λ (nm)[ε × 10^{−3} (M^{−1} cm^{−1})] in CH₂Cl₂: 325 (13.6), 432 (124.0), 547 (6.2), 585 (6.8), 639 (5.2).

Spectroscopy. Proton and ¹³C NMR spectra were recorded at 299.95 (or 599.95) and 75.43 (or 150.87) MHz, respectively, on Varian VXR-300 (or Varian Unity Inova-600) spectrometers locked on deuterated solvent and referenced to the solvent peak. Proton NMR is relative to CD₂Cl₂, CDCl₃, or THF-*d*₈ at δ = 5.30, 7.24, or 1.73 (the upfield resonance) and ¹³C NMR to the center line of CD₂Cl₂, CDCl₃, or THF-*d*₈ at δ = 53.6, 77.0, or 25.3 (the upfield resonance). Next, the temperature of the spectrometer probe was calibrated by the shift difference of methanol resonance in the ¹H NMR spectrum. ¹H–¹³C COSY was used to correlate protons and carbon through one-bond coupling and HMBC (heteronuclear multiple bond coherence) for two- and three-bond proton–carbon coupling.

The positive-ion fast atom bombardment mass spectrum (FAB MS) was obtained in a nitrobenzyl alcohol (NBA) matrix using a JEOL JMS-SX/SX 102A mass spectrometer. UV/visible spectra were recorded at 25 °C on a HITACHI U-3210 spectrophotometer.

Crystallography. Table 1 presents the crystal data as well as other information for Ni(*N-p*-NCOC₆H₄NO₂-tpp) (**1**) and Tl(*N-p*-NCOC₆H₄NO₂-tpp)(OAc) (**3**). Measurements were taken on a Siemens SMART

(6) Huheey, J. E.; Keiter, E. A.; Keiter, R. L. *Inorganic Chemistry*, 4th ed.; Harper Collins College: New York, 1993; p 114.

* To whom correspondence should be addressed.

(1) Li, Y. I.; Chang, C. S.; Tung, J. Y.; Tsai, C. H.; Chen, J. H.; Liao, F. L.; Wang, S. L. *Polyhedron* **2000**, *19*, 413.

(2) Callot, H. J.; Chevrier, B.; Weiss, R. *J. Am. Chem. Soc.* **1978**, *100*, 4733.

(3) Mahy, J. P.; Battioni, P.; Bedi, G.; Mansuy, D.; Fishcher, J.; Weiss, R.; Morgenstern-Badarau, I. *Inorg. Chem.* **1988**, *27*, 353.

(4) Callot, H. J.; Chevrier, B.; Weiss, R. *J. Am. Chem. Soc.* **1979**, *101*, 7729.

(5) Tung, J. Y.; Jang, J. I.; Lin, C. C.; Chen, J. H.; Hwang, L. P. *Inorg. Chem.* **2000**, *39*, 1106.

Table 1. Crystal Data for (1) and (3)

empirical formula	C ₅₁ H ₃₂ N ₆ NiO ₃ (1)	C ₅₃ H ₃₅ N ₆ O ₅ Tl (3)
fw	835.54	1040.24
space group	C2/c	P2 ₁ /c
cryst syst	monoclinic	monoclinic
a, Å	22.5402(11)	12.5257(14)
b, Å	15.7500(8)	24.360(3)
c, Å	22.6703(11)	14.5349(17)
α, deg	90	90
β, deg	96.8100(10)	101.124(2)
γ, deg	90	90
V, Å ³	7991.4(7)	4351.7(9)
Z	8	4
F ₀₀₀	3456	2064
D _{calcd} , g cm ⁻³	1.389	1.588
μ(Mo Kα), cm ⁻¹	5.40	37.70
S	1.058	0.864
cryst size, mm ³	0.8 × 0.3 × 0.2	0.11 × 0.26 × 0.28
2θ _{max} , deg	56.58	52.06
T, K	295(2)	293(2)
no. of reflns measd	23 412	24 296
no. of reflns obsd	8921 (I > 2σ(I))	8546 (I > 2σ(I))
R ^a (%)	4.21	4.45
R _w ^b (%)	11.25	11.47

^a $R = [\sum ||F_o| - |F_c|| / \sum |F_o|]$. ^b $R_w = [\sum w(|F_o| - |F_c|)^2 / \sum w(|F_o|)^2]^{1/2}$; $w = A / (\sigma^2 F_o + BF_o^2)$.

Table 2. Selected Bond Distances (Å) and Angles (deg) for Compounds 1 and 3

Ni(<i>N-p</i> -NCOC ₆ H ₄ NO ₂ -tpp) (1)			
Distances			
Ni(1)–N(1)	1.843(2)	N(1)–C(1)	1.343(2)
Ni(1)–N(3)	1.937(2)	C(1)–O(1)	1.227(2)
Ni(1)–N(4)	1.874(2)	C(1)–C(2)	1.504(3)
Ni(1)–N(5)	1.940(2)	N(1)–N(2)	1.390(2)
Angles			
N(3)–Ni(1)–N(5)	166.39(7)	Ni(1)–N(1)–N(2)	104.8(1)
N(3)–Ni(1)–N(1)	86.92(7)	Ni(1)–N(1)–C(1)	141.2(1)
N(3)–Ni(1)–N(4)	93.87(7)	N(1)–C(1)–O(1)	123.9(2)
N(1)–Ni(1)–N(5)	88.34(7)	N(1)–C(1)–C(2)	116.4(2)
N(1)–Ni(1)–N(4)	164.18(7)	N(4)–Ni(1)–N(5)	94.16(7)
Tl(<i>N-p</i> -NCOC ₆ H ₄ NO ₂ -tpp)(OAc) (3)			
Distances			
Tl–O(4)	2.356(5)	N(5)–N(1)	1.409(6)
Tl–O(5)	2.365(4)	O(4)–C(52)	1.250(8)
Tl–N(2)	2.337(5)	O(5)–C(52)	1.248(8)
Tl–N(3)	2.157(4)	C(52)–C(53)	1.496(9)
Tl–N(4)	2.343(4)	N(5)–C(45)	1.345(7)
Tl–N(5)	2.147(5)	C(45)–O(1)	1.225(7)
Angles			
O(4)–Tl–O(5)	54.9(2)	Tl–O(4)–C(52)	92.0(4)
O(4)–Tl–N(2)	146.9(2)	Tl–O(5)–C(52)	91.6(4)
O(4)–Tl–N(3)	93.2(2)	O(4)–C(52)–O(5)	121.3(6)
O(4)–Tl–N(4)	91.3(2)	Tl–N(5)–C(45)	133.1(4)
O(4)–Tl–N(5)	112.5(2)	Tl–N(5)–N(1)	106.6(3)
O(5)–Tl–N(2)	93.1(2)	O(5)–Tl–N(4)	146.0(2)
O(5)–Tl–N(3)	95.4(2)	O(5)–Tl–N(5)	110.8(2)

CCD diffractometer using monochromatized Mo Kα radiation ($\lambda = 0.71073$ Å). The empirical absorption corrections were made for 1. The structures were solved by direct methods (SHELXTL PLUS) and refined by the full-matrix least-squares method. All non-hydrogen atoms were refined with anisotropic thermal parameters, whereas all hydrogen atom positions were calculated using a riding model and were included in the structure factor calculation. Table 2 lists selected bond distances and angles for both complexes.

Results and Discussion

Molecular Structures of 1 and 3. The X-ray framework is depicted in Figure 1a for the complex Ni(*N-p*-NCOC₆H₄NO₂-

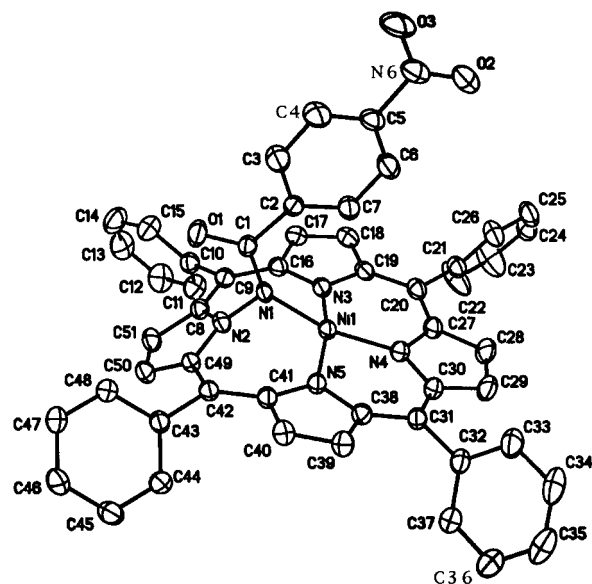
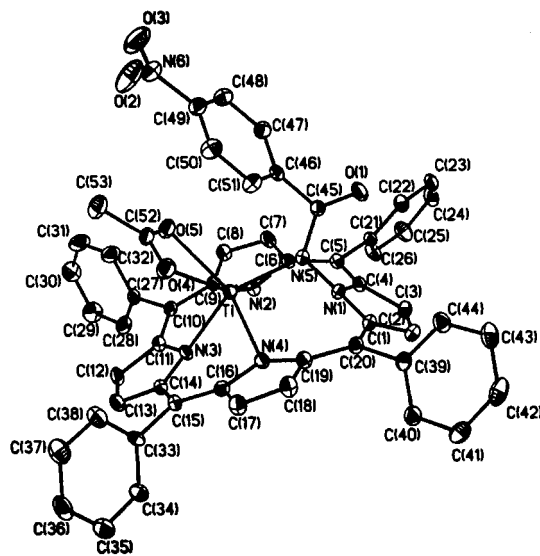
**(a) Ni(*N-p*-NCOC₆H₄NO₂-tpp)****(b) Tl(*N-p*-NCOC₆H₄NO₂-tpp)(OAc)**

Figure 1. Molecular configuration and atom-labeling scheme for (a) Ni(*N-p*-NCOC₆H₄NO₂-tpp) (1) and (b) Tl(*N-p*-NCOC₆H₄NO₂-tpp)(OAc) (3), with ellipsoids drawn at 30% probability. Hydrogen atoms for both compounds are omitted for clarity.

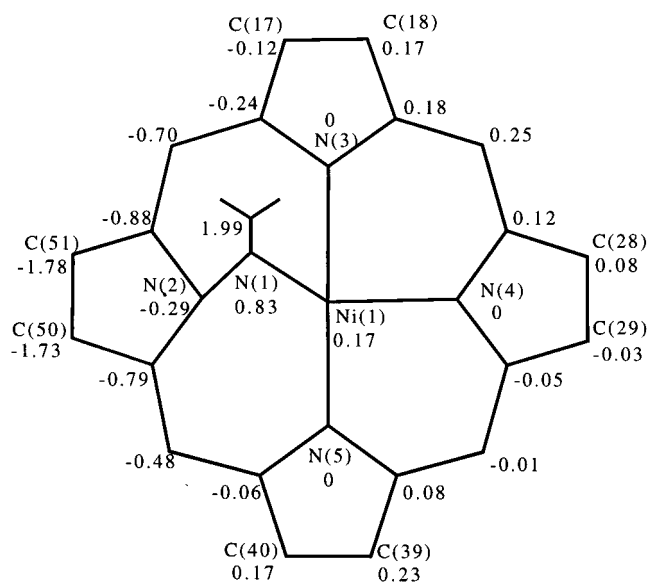
tpp) (1) and in Figure 1b for Tl(*N-p*-NCOC₆H₄NO₂-tpp)(OAc) (3). Both these structures, four-coordinate nickel of 1 and six-coordinate thallium of 3, have bonding with three nitrogen atoms of the porphyrins and one extra nitrogen atom of the nitrene fragment in common, but compound 3 has in addition one more chelating bidentate OAc⁻ ligand in the axial site. In 1 and 3 it appears that the *N-p*-nitrobenzoyl (NB) moiety is inserted into the Ni–N bond of *meso*-tetraphenylporphyrinatonicel(II), Ni(tpp),⁷ and the Tl–N bond of acetato(*meso*-tetraphenylporphyrinato)thallium(III) Tl(tpp)(OAc).⁸ The unusual metal–ligand bond distances, i.e., from Ni(II) and Tl(III) atoms to the ligand, and the angles are summarized in Table 2. The interaction of the acetate with thallium is chelating bidentate. This kind of

(7) Marsh, D. F.; Mink, L. M. *J. Chem. Educ.* 1996, 73, 1188.

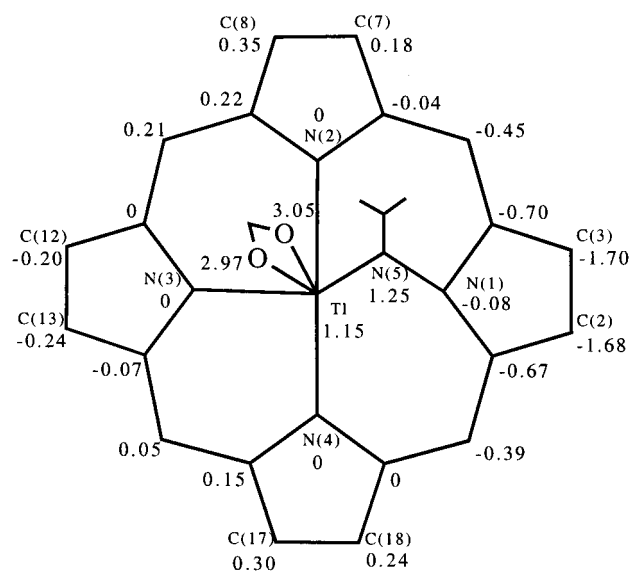
bidentate interaction was previously observed for $\text{Tl}(\text{N-NTs-tpp})(\text{OAc})$ with $\text{Tl}-\text{O}(1) = 2.410(8) \text{ \AA}$ and $\text{Tl}-\text{O}(2) = 2.292(9) \text{ \AA}$.⁵

The geometry around Ni^{2+} is a distorted square planar, whereas for Tl^{3+} it is described as a distorted square-based pyramid in which the apical site is occupied by a chelating bidentate OAc^- group. The pyrrole nitrogens $\text{N}(2)$ and $\text{N}(1)$ are no longer bonded to the nickel and thallium as indicated by their longer internuclear distances, 2.576 \AA for $\text{Ni}(1)\cdots\text{N}(2)$ and 2.886 \AA for $\text{Tl}\cdots\text{N}(1)$. The $\text{Ni}(1)-\text{N}(4)$ bond trans to the $\text{N}(1)$ position in compound **1** is slightly shorter than the other two $\text{Ni}(1)-\text{N}$ bond distances [i.e., $1.874(2) \text{ \AA}$ for $\text{Ni}(1)-\text{N}(4)$, compared to $1.937(2) \text{ \AA}$ for $\text{Ni}(1)-\text{N}(3)$ and $1.940(2) \text{ \AA}$ for $\text{Ni}(1)-\text{N}(5)$]. Similarly, the $\text{Tl}-\text{N}(3)$ bond in compound **3** is also shorter than the other two $\text{Tl}-\text{N}$ distances [$2.157(4) \text{ \AA}$ for $\text{Tl}-\text{N}(3)$ vs $2.343(4) \text{ \AA}$ for $\text{Tl}-\text{N}(4)$ and $2.337(5) \text{ \AA}$ for $\text{Tl}-\text{N}(2)$]. Figure 2 shows the actual porphyrin skeleton of **1** and **3**. We adopt the plane of three strongly bound pyrrole nitrogen atoms [i.e., $\text{N}(3)$, $\text{N}(4)$, and $\text{N}(5)$ for **1** and $\text{N}(2)$, $\text{N}(3)$, and $\text{N}(4)$ for **3**] as a reference plane 3N. Because of the larger size of the Tl^{3+} , Tl and $\text{N}(5)$ lie 1.15 and 1.25 \AA , respectively, above the 3N plane in **3**, compared to 0.17 \AA for Ni and 0.83 \AA for $\text{N}(1)$ in **1** (Figure 2). For the same reason, i.e., due to the larger size of the Tl^{3+} , the chelating bidentate acetate in **3** is cis to the NB group with $\text{O}(4)$ and $\text{O}(5)$ being located separately at 2.97 and 3.05 \AA out of the 3N plane. The porphyrin macrocycle is indeed distorted because of the presence of the NB group (Figure 2). Thus, the $\text{N}(2)$ and $\text{N}(1)$ pyrrole rings bearing the NB group would be deviated mostly from the 3N plane and oriented separately in a dihedral angle of 43.8° and of 49.4° , whereas small angles of 11.4° , 4.5° , and 6.8° occur with $\text{N}(3)$, $\text{N}(4)$, and $\text{N}(5)$ pyrroles for compound **1** and 9.9° , 6.5° , and 8.3° with $\text{N}(2)$, $\text{N}(3)$, and $\text{N}(4)$ pyrroles for compound **3**. In compound **1**, such a large deviation from planarity for the $\text{N}(2)$ pyrrole is also reflected by observing a $12-19$ ppm upfield shift of the C_β ($\text{C}50$, $\text{C}51$) at 118.4 ppm compared to 137.8 ppm for C_β ($\text{C}18$, $\text{C}39$), 133.8 ppm for C_β ($\text{C}28$, $\text{C}29$), and 130.3 ppm for C_β ($\text{C}17$, $\text{C}40$) (Figure S1a in Supporting Information). In compound **3**, a similar deviation is also found for the $\text{N}(1)$ pyrrole by observing a $17-21$ ppm upfield shift of the C_β ($\text{C}2$, $\text{C}3$) at 115.2 ppm compared to 132.3 ppm for C_β ($\text{C}12$, $\text{C}13$), 133.9 ppm for C_β ($\text{C}7$, $\text{C}18$), and 136.0 ppm for C_β ($\text{C}8$, $\text{C}17$). Similar kinds of upfield shifts of C_β resonances due to the nonplanarity of porphyrin were also observed with a magnitude of $15-17$ ppm for $\text{Zn}(\text{N-NTs-tpp})$,¹ $16-21$ ppm for $\text{Tl}(\text{N-NTs-tpp})(\text{OAc})$,⁵ and $5.6-7.0$ ppm for $\text{Tl}(\text{N-Me-tpp})(\text{OAc})_2$.⁹

The pyrrole ring nitrogens $\text{N}(2)$ and $\text{N}(1)$ are in fact inclined toward the Ni and Tl atoms, in **1** and **3**, respectively. These distortions make the distances between opposite pyrrole nitrogen atoms unusual. The normal diameter of the "hole" in an undistorted metalloporphyrin complex has been estimated to be 4.02 \AA .¹⁰ The $\text{N}(2)\cdots\text{N}(4)$ distance of 4.409 \AA in **1** and the $\text{N}(1)\cdots\text{N}(3)$ distance of 4.439 \AA in **3** are unusually long, which is caused by the large deviations of the $\text{N}(2)$ pyrrole in **1** and $\text{N}(1)$ pyrrole in **3** from the 3N plane, respectively. Also affected by the distortion are the $\text{N}(3)\cdots\text{N}(5)$ distance of 3.849 \AA in **1** and the $\text{N}(2)\cdots\text{N}(4)$ distance of 4.039 \AA in **3**. Hence, in **3**, the thallium(III) atom is bound in an expanded porphyrinato (4N) core [i.e., the plane $\text{N}(1)-\text{N}(4)$]. The plane (P) defined by Ni ($\text{N}(1)$, $\text{N}(2)$, and $\text{C}(1)$) in **1**, and by Tl , $\text{N}(5)$, $\text{N}(1)$, and $\text{C}(45)$



(a) $\text{Ni}(\text{N-p-NCOC}_6\text{H}_4\text{NO}_2\text{-tpp})$



(b) $\text{Tl}(\text{N-p-NCOC}_6\text{H}_4\text{NO}_2\text{-tpp})(\text{OAc})$

of (a) compound **1** and (b) compound **3**. The values represent the displacements (in angstroms) of the atoms from the mean 3N plane [i.e., $\text{N}(3)-\text{N}(5)$ for **1** and $\text{N}(2)-\text{N}(4)$ for **3**].

in **3** is almost perpendicular to the 3N plane with a angle of 87.3° for **1** and 81.4° for **3**. The *p*-nitrobenzoyl group (NB) [i.e., the plane for NB in **1** is $\text{C}(2)-\text{C}(7)$ and for **3** it is $\text{C}(46)-\text{C}(51)$] is bonded to $\text{N}(1)$ in **1** and $\text{N}(5)$ in **3** so that it lies above the macrocycle, orienting in a dihedral angle of 85.6° and 68.2° with the 3N plane in **1** and **3**, respectively. The dihedral angles between the mean plane of the skeleton (3N) and the planes of the phenyl groups are 59.8° [$\text{C}(13)$], 69.7° [$\text{C}(24)$], 64.0° [$\text{C}(35)$], and 36.9° [$\text{C}(46)$] for **1** and 44.0° [$\text{C}(24)$], 78.7° [$\text{C}(30)$], 87.4° [$\text{C}(36)$], and 42.2° [$\text{C}(42)$] for **3**.

The comparison made for $\text{Ni}(\text{II})$ derivatives of carbene, nitrene, and oxygen inserted complexes displays severe nonplanarity. $\text{Ni}(1)$ and $\text{N}(1)$ lie 0.23 and 1.01 \AA above the mean plane of the four pyrrole nitrogens $\text{N}(2)-\text{N}(5)$ (i.e., 4N plane) in **1** compared to 0.19 \AA for Ni and 1.04 \AA for the extra carbon atom $\text{C}1$ of the ethoxycarbonylcarbene fragment inserted into

(8) Suen, S. C.; Lee, W. B.; Hong, F. E.; Jong, T. T.; Chen, J. H.; Hwang, L. P. *Polyhedron* **1992**, *11*, 3025.

(9) Tung, J. Y.; Chen, J. H.; Liao, F. L.; Wang, S. L.; Hwang, L. P. *Inorg. Chem.* **2000**, *39*, 2120.

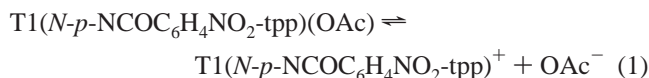
(10) Collins, D. M.; Hoard, J. L. *J. Am. Chem. Soc.* **1970**, *92*, 3761.

a Ni–N bond of nickel(II) *meso*-tetraphenylporphine.¹¹ Additionally, Ni(1) and N(1) lie 0.17 and 0.83 Å above the 3N plane in **1** compared to 0.05 Å for Ni and 0.65 Å for O(1) in nickel(II) octaethylporphyrin *N*-oxide.¹² The nonplanarity is further reflected in the angle between the 4N plane and the N(2) pyrrole ring in **1**. This angle is 39.9° for **1** compared to 46.4° for the N(4) pyrrole ring in the complex with an ethoxycarbonylcarbene moiety inserted into a Ni–N bond of nickel(II) *meso*-tetraphenylporphine.¹¹ Furthermore, the angle between the plane of the N(2) pyrrole ring and the 3N plane is 43.8° in **1**, while that between the plane of *N*-oxide pyrrole and the plane of the other three pyrrole and the two connecting meso carbons is 38.3° in nickel(II) octaethylporphyrin *N*-oxide.¹²

¹H and ¹³C NMR for Ni(*N-p*-NCOC₆H₄NO₂-tpp) (1**) and Tl(*N-p*-NCOC₆H₄NO₂-tpp)(OAc) (**3**) in CDCl₃ and CD₂Cl₂ (Figure S1 in Supporting Information).** In solution, the molecule has effective C_s symmetry with a mirror plane running through the N(4)–Ni(1)–N(1)–N(2) unit for **1** or the N(3)–Tl–N(5)–N(1) unit for **3**. There are four distinct β-pyrrole protons H_β, four β-pyrrole carbons C_β, four α-pyrrole carbons C_α, two different meso carbons C_{meso}, and two phenyl-C₁ carbons for both complexes. The NMR study of **3** showed four different types of Tl–H coupling constants for H_β (Figure S1b in Supporting Information). The doublet at 8.63 ppm is assigned as H_β(12,13) with ⁴J(Tl–H) = 75.3 Hz, and the doublet at 7.20 ppm is due to H_β(2,3) with ⁵J(Tl–H) = 6 Hz. The doublet of a doublet at 9.32 ppm is due to H_β(8,17) with ⁴J(Tl–H) = 20 Hz and ³J(H–H) = 4.5 Hz, and the doublet of a doublet at 8.96 ppm is due to H_β(7,18) with ⁴J(Tl–H) = 14 Hz and ³J(H–H) = 4.8 Hz. Likewise, there were also four different types of Tl–¹³C coupling constants for C_β. The doublet at 132.3 ppm is due to C_β (C12, C13) with ³J(Tl–¹³C) = 167 Hz, and the doublet at 136.0 ppm is due to C_β (C8, C17) with ³J(Tl–¹³C) = 39 Hz. The singlet at 133.9 ppm is due to C_β (C7, C18) with ³J(Tl–¹³C) being unobserved and the doublet at 115.2 ppm is due to C_β (C2, C3) with ⁴J(Tl–¹³C) = 82 Hz. The ¹H NMR spectra reveal that the aromatic protons of the NB group appear as a doublet at 7.04 (NB-H_{3,5}) and triplet at 5.25 ppm (NB-H_{2,6}) for **3** (Figure S1b in Supporting Information) and at 6.80 (d) and 4.93 (t) ppm for **1**. All *p*-nitrobenzoylimido and acetato protons are shifted upfield compared to their counterparts in free *N-p*-HNC₆H₄NO₂-Htpp and OAc[−]; such a shift is presumably attributed to the porphyrin ring current effect. The ring current effect indicates that the NB groups are bonded to Ni(1) in **1** and to Tl in **3**. This bonding argument is further supported by the result that in ¹³C NMR the NB-C₁ [i.e., C(46)] and the C(45) in **3** were observed at 138.9 ppm with ³J(Tl–C) = 22 Hz and at 168.2 ppm with ²J(Tl–C) = 599 Hz, respectively. Because C(45) in **3** is bonded to an electronegative atom O(1), the 2p-electron density around carbon C(45) is reduced. This removal of electron density increases both the effective nuclear charge and the s-electron density for the C(45) nucleus, and therefore ²J(Tl–C) coupling constants increase from 65 ± 24 Hz for C_α to 599 Hz for C(45) in **3**.¹³

Dynamic NMR of **3 in THF-*d*₈.** Upon cooling of a 3.6 × 10^{−3} M THF-*d*₈ solution of **3** (Figure S2 in Supporting Information), the methyl proton signals of OAc[−] are a single peak at 25 °C (δ = 0.16 ppm), first broadened (coalescence temperature T_c = −98 °C) and then split into two peaks with a

separation of 18 Hz at δ = 0.034 ppm at −110 °C. As the exchange of OAc[−] within **3** is reversible, the results at 599.95 MHz confirm the separation as a coupling of ⁴J(Tl–H) rather than a chemical shift difference. The most likely cause of loss of coupling is due to reversible dissociation of acetate



with a small dissociation constant.¹⁴ Such a scenario would lead to a change in the chemical shift with temperature and no detectable free OAc[−] and Tl(*N-p*-NCOC₆H₄NO₂-tpp)⁺ at low temperature, but would lead to the loss of coupling between acetate and thallium at higher temperature. The chemical shift in the high-temperature limit is the average of the two species [i.e., Tl(*N-p*-NCOC₆H₄NO₂-tpp)(OAc) and OAc[−]] in eq 1 weighted by their concentration. A comparison of observed and computed spectra yields ΔG[‡]₁₇₅ = 36.7 kJ/mol. At 25 °C, intermolecular exchange of the OAc[−] group is rapid as indicated by the appearance of singlet signals due to carbonyl carbons at 175.1 ppm and methyl carbons at 18.5 ppm. At −110 °C, the rate of intermolecular exchange of OAc[−] for **3** in THF-*d*₈ is slow. Hence, at this temperature, the methyl and carbonyl carbons of OAc[−] are observed at 18.9 ppm [with ³J(Tl–C) = 227 Hz] and 175.9 ppm [with ²J(Tl–C) = 211 Hz] as doublets, respectively. These ¹³C resonances are quite close to that of Tl(*N*-NTs-tpp)(OAc) in which the two corresponding carbons were also observed, in CD₂Cl₂ at −110 °C, at 18.5 ppm [with ³J(Tl–C) = 220 Hz] and 176.3 ppm [with ²J(Tl–C) = 205 Hz] as doublets.⁵

At low temperature, some differences in OAc[−] resonances were observed. However, the differences for the ¹H resonances of pyrrole protons H_β, meta and para protons in porphyrin, and the resonances of NB-H_{2,6} and NB-H_{3,5} in *N-p*-nitrobenzoylimido were small for **3** in THF-*d*₈ at 25 and −110 °C. However, for ortho protons, at −110 °C, the rotation of phenyl group along the C₁–C_{meso} bond in **3** is slow, which is evident from the appearance of the four broad singlets at 8.94, 8.31, 8.17, and 8.06 ppm due to four different ortho protons of the aromatic ring. At 25 °C, this rotation becomes more rapid, and hence the ¹H resonances for ortho protons of **3** were observed in THF-*d*₈ with two sets of doublet and one broad singlet: one doublet at 8.22 ppm with ³J(H–H) = 6 Hz and the other doublet at 8.13 ppm with ³J(H–H) = 7.2 Hz, and one broad singlet at 8.54 ppm.

Though we did not undertake the experiment to observe the OAc[−] exchange with O¹³Ac[−], PrO[−], or PhCOO[−], a similar kind of intermolecular OAc[−] (or benzoate) exchange was also observed for Tl(*N*-Me-tpp)(OAc)₂⁹ in THF-*d*₈ [or for Tl(tmp-p)(PhCOO) in CD₂Cl₂ solvent].¹⁵ From the above analysis, the exchange of OAc[−] in **3** should be an intermolecular process. To date, other anions such as Cl[−], N₃[−], and MeO[−] cannot behave as ligands of the cationic thallium complex Tl(*N-p*-NCOC₆H₄NO₂-tpp)⁺.

The properties of complex **1** in the solid state are similar to those properties in solution. However, for **3**, the properties in the solid state are different from those in solution, because complex **3** dissociates into Tl(*N-p*-NCOC₆H₄NO₂-tpp)⁺ and OAc[−] in THF solution.

(11) Chevrier, B.; Weiss, R. *J. Am. Chem. Soc.* **1976**, *98*, 2985.

(12) Balch, A. L.; Chan, Y. W.; Olmstead, M. M. *J. Am. Chem. Soc.* **1985**, *107*, 6510.

(13) Wehri, F. W.; Marchand, A. P.; Wehri, S. *Interpretation of Carbon-13 NMR Spectra*, 2nd ed.; John Wiley & Sons: New York, 1989; pp 65–66.

(14) Jenson, J. P.; Muetterties, E. L. In *Dynamic Nuclear Magnetic Resonance Spectroscopy*; Jackman, L. M., Cotton, F. A., Eds.; Academic Press: New York, 1975; pp 299–304.

(15) Sheu, Y. H.; Hong, T. N.; Chen, J. H.; Liao, F. L.; Wang, S. L.; Wang, S. S.; Yang, C. T. *Polyhedron* **1997**, *16*, 1621.

Conclusions

We have investigated for the first time the two diamagnetic, mononuclear, and bridged metal complexes of *N-p*-nitrobenzoylamido-*meso*-tetraphenylporphyrin having M-*N*-(*p*-COC₆H₄-NO₂)-N [or M-*N*-NB-N, M = Ni(II), Tl(III)] linkage, and their X-ray structures are analyzed. Excepting the phenyl protons and carbons, the unambiguous assignments of ¹H and ¹³C NMR data for **1** in CDCl₃ and **3** in CD₂Cl₂ are reported in this work. Dynamic ¹H and ¹³C NMR spectra of the acetato group in **3** reveal that this group undergoes an intermolecular exchange with a free energy of activation, $\Delta G_{175}^{\ddagger} = 36.7$ kJ/mol.

Acknowledgment. The financial support from the National Science Council of the R.O.C. under Grant NSC 89-2113-M-005-023 is gratefully acknowledged.

Supporting Information Available: ¹³C NMR spectrum (Figure S1) and its assignment for **1**, ¹H NMR spectrum of **3** (Figure S1) and its ¹³C NMR data and ¹H NMR spectra for the acetato protons of **3** (Figure S2) at various temperatures; X-ray crystallographic files in CIF format for compounds **1** and **3**. This material is available free of charge via the Internet at <http://pubs.acs.org>.

IC000823P